Numerical investigation of bio-inspired tubular composite to steel joints

E. I. Avgoulas[1*], M. P. F. Sutcliffe[1]

[1]Department of Engineering, University of Cambridge, Trumpington Street,
Cambridge, CB2 1PZ United Kingdom
*eia21@cam.ac.uk

Keywords: tubular joints, hybrid, composite, steel, biomimetics.

Abstract

In many high-performance applications there is a need to join tubular steel and composite parts. Bonded joints between dissimilar tubular members under axial tension develop relatively high stresses with steep gradients localised at the joint ends. This is due to the large stiffness mismatch between the materials of the adherends. This paper uses the biomimetics approach to help develop solutions to this problem. One of the key methods that nature uses to join dissimilar materials is a transitional zone of stiffness at the insertion site. This method was used to propose bio-inspired solutions with a transitional zone of stiffness at the joint site for tubular CFRP-to-steel and GFRP-to-steel adhesively bonded joint configurations. The transition zone was used to reduce the material stiffness mismatch of the joint parts. Two-dimensional axisymmetric finite-element models of tubular CFRP-to-steel and GFRP-to-steel joints were developed. A cohesive zone degradation formulation was chosen to calculate accurately the load carrying capacity of the adhesive joints. The model was used to identify the optimum variation in material stiffness which minimises potential failure of the joint. The best bio-inspired CFRP-to-steel and GFRP-to-steel joints showed a 10% and 30% increase of joint strength comparing to the non-bioinspired ones.

1. Introduction

Nowadays, many of the modern turboprop engines in operation are equipped with carbon fibre reinforced plastic (CFRP) propeller blades. World-leading manufacturers of integrated propeller systems use CFRP to steel tubular joints to attach the CFRP blade to the steel hub. Applications range from regional airliners (e.g. Bombardier’s twin-engine Q400 Dash 8) and military airlifters (e.g. Lockheed Martin’s four-engine C-130J) to marine hovercraft (Textron Systems’ Landing Craft Air Cushion (LCAC) hovercraft). Additionally, composite tubular structures are used in piping systems with applications in a wide range of industries (e.g. aerospace, marine, chemical). Composite materials are an attractive alternative to metals considering the extreme environments that the piping systems are exposed in onshore or offshore applications [1].

The idea of a transitional zone of stiffness between dissimilar materials used by natural joint designs was adapted to tubular adhesively bonded hybrid joints. The aim is to evaluate the hypothesis that using the bio-inspired design strategy of a transitional zone of stiffness across the overlap length of

Excerpt from ISBN 978-3-00-053387-7

tubular CFRP-to-steel and glass fibre reinforced plastic (GFRP) to steel joints can increase the strength of the joints.

2. Finite element modelling

Two-dimensional axisymmetric finite-element models of tubular CFRP-to-steel and GFRP-to-steel joints were developed (Figure 1). Figure 1 shows the geometry of the model, which follows the geometric characteristics of the CFRP to perforated steel joint investigated in [2], but in a two-dimensional axisymmetric concept with an internal diameter equal to 89.7 mm. The composite and steel adherends were modelled with elastic orthotropic and isotropic material properties, respectively. The Young's modulus of the steel material was taken as 200 GPa and the Poisson's ratio as 0.28. The composite part of the joints was modelled as a unidirectional CFRP and GFRP material with a Young's modulus in the principal axis 1 (loading direction) E_{1CFRP} = 100 GPa and E_{1GFRP} = 20 GPa, respectively. Bilinear 4-node axisymmetric quadrilateral elements (CAX4I) available in the ABAQUS® library were used for the adherends. Cohesive zone elements were used for the simulation of the adhesive layer to calculate accurately the load carrying capacity of the adhesive joints [3, 4]. A triangular cohesive zone degradation formulation was chosen because of its simplicity, widespread use for investigation purposes, especially for brittle adhesives [5], and availability in ABAQUS®. The adhesive layer was modelled with a single layer of 4-node axisymmetric cohesive elements (COHAX4) with a thickness of 0.2 mm. A displacement u_x was applied to the steel end of the model.

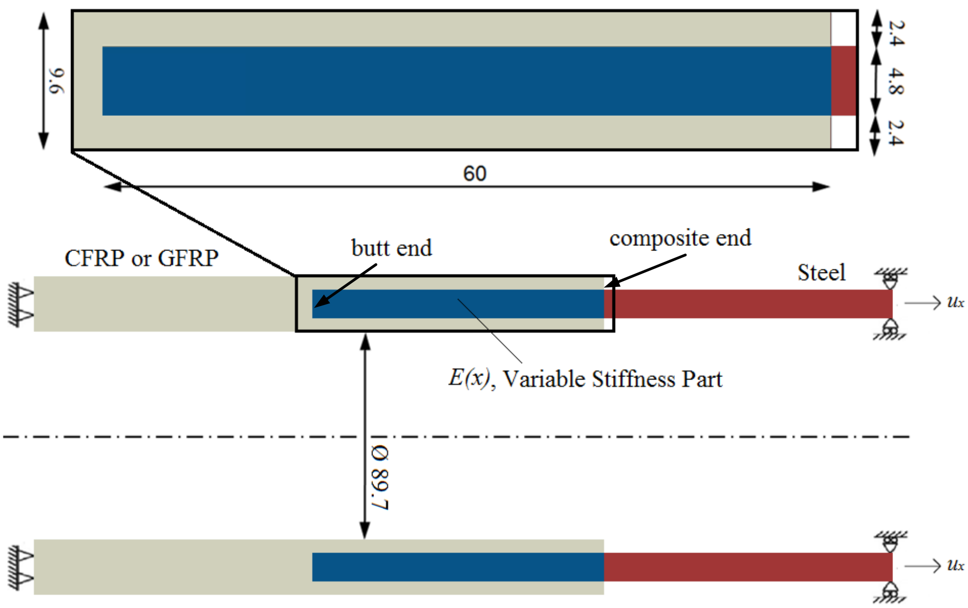

Figure 1. Axisymmetric tubular joint geometry (dimensions in mm), loading and boundary conditions.

The proposed solutions offered a transitional zone of stiffness in the overlap region of the metal part to reduce the material stiffness mismatch at the joint site (see Figure 1). Different sets of variable stiffness functions were investigated to optimise the material stiffness variation, identifying the stiffness function which minimises potential failure of the joint. The stiffness *E(x)* of the metal part

Excerpt from ISBN 978-3-00-053387-7

was varied as a function of the position x along the overlap region of the joint, from a minimum value of E_{Smin} at the butt end of the joint, to a maximum value of E_{Smax} at the composite end of the joint. The value of E_{Smax} was held fixed at 200 GPa, while E_{Smin} was chosen to take values of 10, 20, 40, 70 or 100 GPa, depending on the composite adherend investigated (Table 1). The variation within the overlap between these extreme stiffnesses at the two ends was described using s-shaped functions as described by equation 1.

$$E(x) = E_{Smin} + \frac{E_{Smax} - E_{Smin}}{1 + e^{-a\left(x - x_c/2\right)}} \tag{1}$$

where x_c is the overlap length. The locations with x = 0 and 60 mm correspond to the butt end and composite end of the overlap length, respectively. Figure 2 illustrates the resulting stiffness variations within the overlap length for the chosen values of a. The user subroutine USDFLD in ABAQUS® was used to implement the stiffness variation along the overlap length in the finite element model. For comparison, reference joints were modelled with the same configurations but without any stiffness variation.

Table 1. Configurations investigated.

Test	**Materials**	**Stiffness variation in the steel part (GPa)**	**Stiffness function type**
REF hybrid$_{CFRP}$	Steel-to-CFRP	none (constant stiffness of 200)	none
REF hybrid$_{GFRP}$	Steel-to-GFRP		
hybrid joints	Steel-to-CFRP	100 to 200	s-shaped (all a-values)
		70 to 200	
		40 to 200	
hybrid joints	Steel-to-GFRP	40 to 200	s-shaped (all a-values)
		20 to 200	
		10 to 200	

Excerpt from ISBN 978-3-00-053387-7

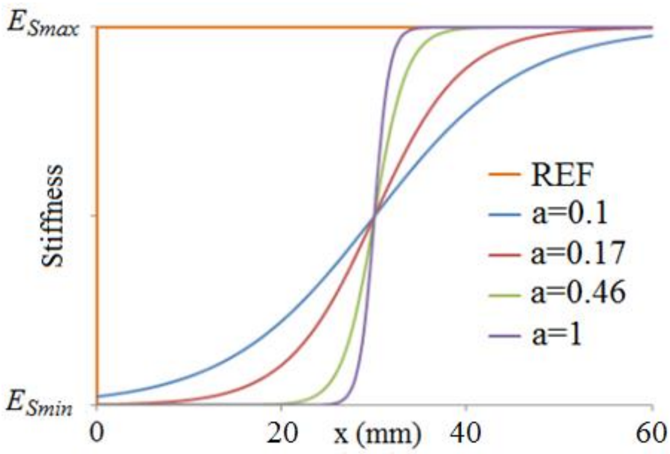

Figure 2. S-shaped functions used to define the variable stiffness of the steel within the overlap length for the chosen values of *a*. The steel stiffness varies from E_{Smin} (which is a variable parameter) to E_{Smax} (which is always equal to 200 GPa).

3. Results and discussion

Figures 3 and 4 summarise the results for the axisymmetric joint configurations of the predicted failure strength, for the s-shaped stiffness distribution in the overlap region, for CFRP-to-steel and GFRP-to-steel joints, respectively. Results for different values of the minimum stiffness E_{Smin} and *a* shape parameter are plotted and compared with the reference configuration without stiffness variation. A set of curves giving the variation of strength with stiffness reduction are given for the chosen range of values of the shape parameter *a*, following the colour key defined by Figure 2.

Figures 3 and 4 show there is an effect of the form of the s-shaped stiffness variation on the strength of the axisymmetric joints. Figure 3 shows that, as the E_{Smin} value is reduced below the stiffness of the CFRP adherend, the strength of the joint is reduced significantly. Axisymmetric hybrid CFRP-to-steel joints with the stiffness in the overlap varying from 100 to 200 GPa (E_{Smin}/E_{Smax} equal to 50%) and following the s-shaped function with $a = 1$ show a 10% increase of the maximum load compared to the reference joints. From Figure 4, it can be seen that the joint strength increases as the reduced stiffness of the steel adherend approaches the stiffness of the GFRP adherend. Axisymmetric hybrid GFRP-to-steel joints with the stiffness in the overlap varying from 20 to 200 GPa (E_{Smin}/E_{Smax} equal to 10%) and following the s-shaped function with $a = 1$ show a 30% increase of the maximum load compared to the reference joints.

Excerpt from ISBN 978-3-00-053387-7

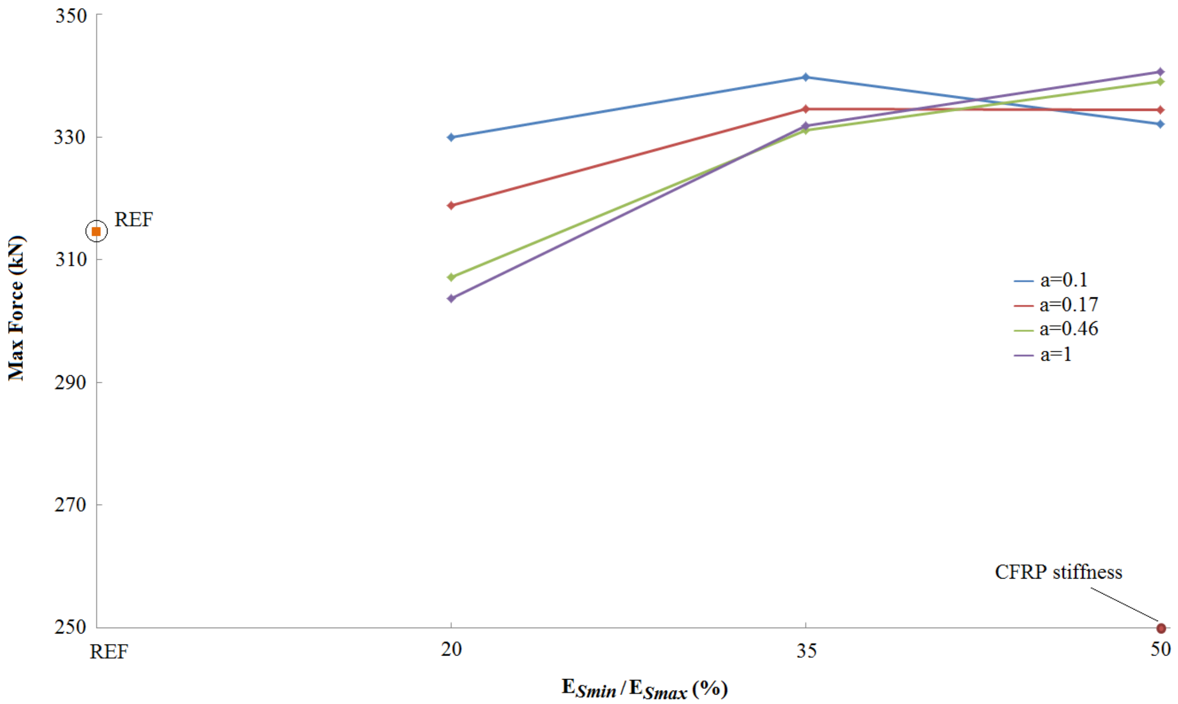

Figure 3. Comparison of the numerical maximum load between reference (REF) and bio-inspired joints with s-shaped stiffness variations; CFRP-to-steel joints.

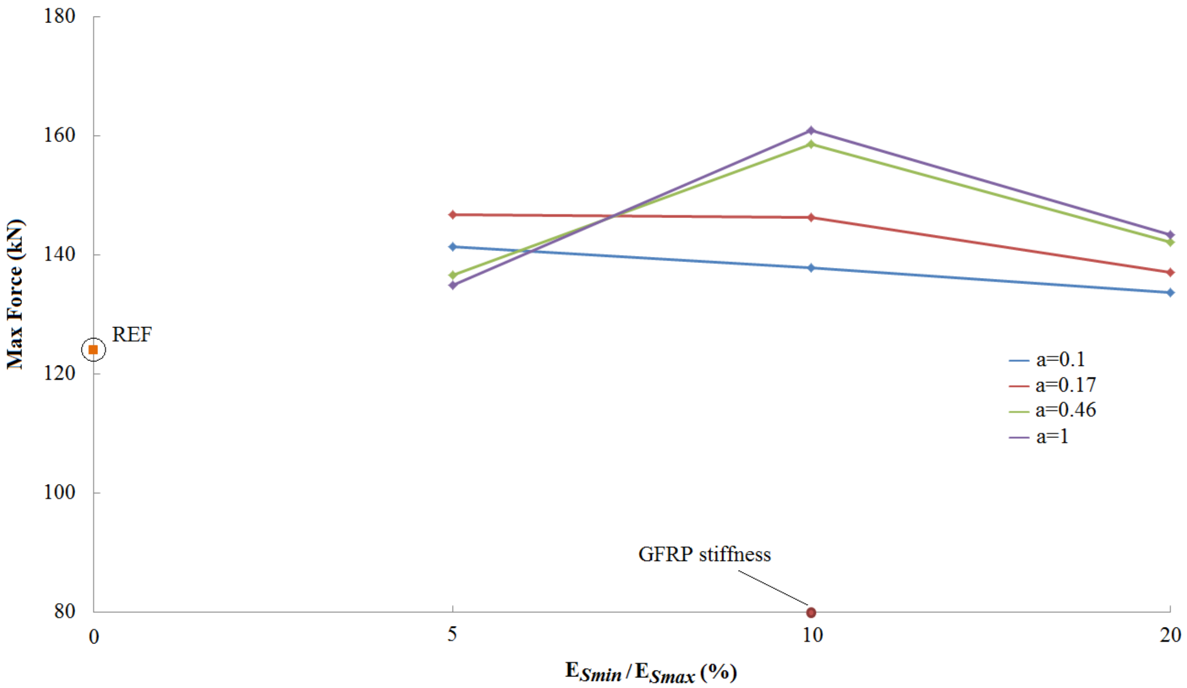

Figure 4. Comparison of the numerical maximum load between reference (REF) and bio-inspired joints with s-shaped stiffness variations; GFRP-to-steel joints.

Excerpt from ISBN 978-3-00-053387-7

4. Conclusions

In this paper the bio-inspired idea of a transitional zone of stiffness between dissimilar materials was numerically investigated in tubular CFRP-to-steel and GFRP-to-steel joint configurations. An optimisation procedure was carried out to identify the material stiffness variation within the steel overlap region which gives the joint with the highest strength. Compared to the ideal reference joints, bio-inspired tubular CFRP-to-steel and GFRP-to-steel joints showed a 10% and 30% increase of joint strength for the best case, respectively.

Acknowledgements

The authors acknowledge the financial support provided by Engineering and Physical Sciences Research Council (EPSRC) and Dowty Propellers (part of GE Aviation).

References

[1] Lees, J.M., 2006. Behaviour of GFRP adhesive pipe joints subjected to pressure and axial loadings, Composites: Part A 37, pp. 1171-1179.

[2] Avgoulas, E.I., Sutcliffe, M.P.F., 2015. Numerical and experimental investigation of CFRP to perforated steel joints. Proceedings of the ICCM20, Copenhagen, Denmark, 19-24 July 2015 (keynote presentation).

[3] Anyfantis, K.N., Tsouvalis, N.G., 2012. A novel traction–separation law for the prediction of the mixed mode response of ductile adhesive joints, International Journal of Solids and Structures 49, pp. 213-226.

[4] Campilho, R.D.S.G., Banea, M.D., Neto, J.A.B.P., da Silva L.F.M., 2013. Modelling adhesive joints with cohesive zone models: effect of the cohesive law shape of the adhesive layer. Journal of Adhesion & Adhesives 44, pp. 48-56.

[5] Campilho, R.D.S.G., Banea, M.D., Pinto, A.M.G., da Silva, L.F.M., de Jesus, A.M.P., 2011. Strength prediction of single- and double-lap joints by standard and extended finite element modelling. Int. J. Adhes. Adhes. 31, pp. 363-372.

Excerpt from ISBN 978-3-00-053387-7